

# Sparse differential connectivity graph of scalp EEG for epileptic patients

L. Amini<sup>1,2</sup>, S. Achard<sup>1</sup>, C. Jutten<sup>1</sup>, H. Soltanian-Zadeh<sup>2,3</sup>  
G.A. Hossein-Zadeh<sup>2</sup>, O. David<sup>4</sup>, L. Vercueil<sup>4</sup> \*

1- Laboratory of Grenoble Image Parole Signal Automatique (GIPSA-LAB), INPG, Domaine universitaire- BP 46, F-38402 Grenoble Cedex, France.

2- Control and Intelligent Processing Center of Excellence (CIPCE), Electrical and Computer Engineering Department, Faculty of Engineering, University of Tehran, Tehran, Iran.

3- Radiology Image Analysis Laboratory, Henry Ford Health System, Detroit, MI 48202 USA.

4- INSERM, U836, Grenoble Institut des Neurosciences (GIN), Grenoble University Hospital (CHUG), 38043 Grenoble, France.

**Abstract.** The aim of the work is to integrate the information modulation of the inter-relations between EEG scalp measurements of two brain states in a connectivity graph. We present a sparse differential connectivity graph (SDCG) to distinguish the effectively modulated connections between epileptiform and non-epileptiform states of the brain from all the common connections created by noise, artifact, unwanted background activities and their related volume conduction effect. The proposed method is applied on real epileptic EEG data. Clustering the extracted features from SDCG may present valuable information about the epileptiform focus and their relations.

## 1 Introduction

Connectivity analysis using scalp EEG or fMRI data have been done based on different measures in the literature. The prominent among these measures are synchronization likelihood [1], correlation coefficients [2], coherence [3], and granger causality [4]. Furthermore, several types of evidences have been suggested in the literature proposing some measures to characterize topographical properties of the networks [2, 5]. There are also interests in simultaneous EEG and fMRI connectivity [5, 6].

In this paper, we present a sparse differential connectivity graph (SDCG) to study the relation between electrodes in two brain states based on the maximal overlap discrete wavelet transform (MODWT) [7], wavelet correlation estimation [2, 8] by means of connectivity measure, and multiple hypothesis t-test. In particular we address whether it is possible to benefit from connectivity graphs on scalp EEG for characterization of epileptiform sources.

The paper is organized as follows. In Section 2, we describe the background, and the proposed approach. Section 3 is devoted to the experimental results of the proposed method. Concluding remarks are presented in Section 4.

---

\*We gratefully acknowledge Frédéric Grouiller for acquiring the data of this study.

## 2 Material and methods

### 2.1 Epilepsy

In epilepsy an area of the brain begins to discharge abnormally during a sudden and recurrent attack called seizure. Between two seizures, interictal epileptiform discharges (IED) may appear in the EEG measurements. The IEDs are waves or complexes (defined by International Federation of Societies for Electroencephalography and Clinical Neurophysiology (IFSECN), 1974) discriminated from background activity. Since the appearance of IED has low probability, their quantitative analysis is rather challenging.

### 2.2 MODWT correlation estimation

In this purpose, wavelet correlation [8, 9] has been used as a measure of connectivity. The estimation of this measure is carried out utilizing the maximal overlap discrete wavelet transform (MODWT) [7], which is similar to discrete wavelet transform, but the signal is not subsampled and instead the filters are upsampled at each scale.

Suppose  $d_j^{s_1}[k]$  and  $d_j^{s_2}[k]$  are the  $j$ th level MODWT coefficients of two stochastic processes with zero-mean stationary Gaussian backward differences ( $s_1[k]$  and  $s_2[k]$ ) [10]. The MODWT estimator of the cross-correlation of  $s_1[k]$  and  $s_2[k]$  at scale  $j$  is:

$$\hat{\rho}_{s_1 s_2(j)} = \frac{\hat{Cov} \{d_j^{(s_1)}[k], d_j^{(s_2)}[k]\}}{\sqrt{\hat{Var}(d_j^{(s_1)}[k])\hat{Var}(d_j^{(s_2)}[k])}} \quad (1)$$

where  $\hat{Cov}$  and  $\hat{Var}$  [8, 10] are the estimations of covariance and variance respectively. This estimation is asymptotically normally distributed with characterized confidence interval [10].

### 2.3 Proposed method

The flowchart of the proposed method has been shown in Fig. 1.

1. **EEG data preprocessing:** Since our final project is simultaneous EEG and fMRI analysis, the EEG data was recorded inside the MR scanner. The first preprocessing step is to remove MR artifact using the method introduced in [11]. Next the expert neurologist labels the cleaned data by determining the start and end time points of IED occurrences as IED labels and time intervals without any IED as Non-IED labels. At the end, the 2-4 Hz MODWT coefficients of cleaned data are segmented using these labels.

We have experimentally found 2-4 Hz wavelet coefficients as the best representing features of IED signals. The advantages of wavelet cross-correlation over Fourier cross-correlation has been cited in [8]. Moreover low frequency

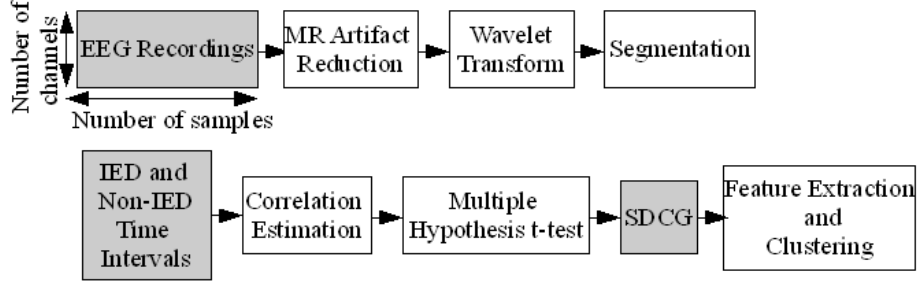


Fig. 1: Flowchart of the proposed method. The EEG preprocessing (top), graph computation and characterization (bottom).

trends of the EEG data, which have unwanted effects on correlation estimation, can be easily removed by wavelet decomposition.

## 2. Graph computation and characterization:

*MODWT Correlation estimation:* The MODWT cross-correlation estimation described in section 2.2 has been used to calculate the correlation coefficients between each pair channels of IED (Non-IED) segments denoted as  $\mathbf{c}_l^{\text{IED}}[k]$  ( $\mathbf{c}_l^{\text{Non-IED}}[k]$ )  $\in \mathbb{R}^{1 \times N_C}$ ,  $k = \{1, 2, \dots, N_C\}$ ,  $l = \{1, 2, \dots, N_L\}$  where  $N_C$ , and  $N_L$  are respectively number of possible connections, and number of IED (Non-IED) labels. The matrix of row concatenation of  $\mathbf{c}_l^{\text{IED}}[k]$  ( $\mathbf{c}_l^{\text{Non-IED}}[k]$ ) vectors, i.e. wavelet correlation of all the connections and all the time IED (Non-IED) labels are denoted as  $\mathbf{I}^{\text{IED}}[k]$  ( $\mathbf{I}^{\text{Non-IED}}[k]$ ).

*Reference sensitivity reduction and multiple hypothesis t-test (MHT):* By thresholding matrix of wavelet correlation,  $\mathbf{I}^{\text{IED}}[k]$  ( $\mathbf{I}^{\text{Non-IED}}[k]$ ) the common connectivity graph [2] for IED (Non-IED) state will be obtained (two separate graphs for each state). These common graphs have several problems in our application: (1) To obtain a sparse graph, thresholding is needed, and the graph depends on the thresholding; (2) The neighborhood nodes are connected due to the volume conduction effect; (3) Comparing two separate connectivity graphs of two brain states to determine the distinguished connections is rather challenging. These problems have been solved by applying multiple hypothesis t-test between  $\mathbf{I}^{\text{IED}}[k]$  and  $\mathbf{I}^{\text{Non-IED}}[k]$ . For each connection a t-test upon the following hypothesis is carried out:

$$\begin{cases} H_0^t : & \mu_1^t = \mu_2^t \\ H_1^t : & \mu_1^t \neq \mu_2^t \end{cases} \quad (2)$$

where  $t = 1, \dots, N_C$ , and  $\mu_i$  is the mean of IED ( $i = 1$ ) and Non-IED ( $i = 2$ ) groups. The non-zero  $t$ -values construct the SDCG. We separated the positive and negative  $t$ -values for better analysis. The positive (negative)  $t$ -values construct positive (negative)  $t$ -value graph. A connection in positive (negative)  $t$ -value graph shows the increase of wavelet correlations in IED (Non-IED) time intervals.

A problem regarding the effect of the EEG reference (EEG data of a specific reference is the subtraction of all the channels from that reference) is the sensitivity of the connectivity graph to the reference. If we calculate the  $\mathbf{I}^{\text{IED}}[k]$  ( $\mathbf{I}^{\text{Non-IED}}[k]$ ) matrix for two different references, the resulted graphs are not exactly the same, but not completely different. To solve this problem, the  $\mathbf{I}^{\text{IED}}[k]$  ( $\mathbf{I}^{\text{Non-IED}}[k]$ ) matrix is calculated for all possible references. Row concatenation of these matrices is denoted as  $\mathbf{R}^{\text{IED}}[k]$  ( $\mathbf{R}^{\text{Non-IED}}[k]$ ). Then the MHT is applied between  $\mathbf{R}^{\text{IED}}[k]$  and  $\mathbf{R}^{\text{Non-IED}}[k]$ . The resulted graph gives the significant robust connections between the two brain states (IED and Non-IED) by considering the temporal and spatial information.

*Feature extraction and clustering:* The nodes of the resulted SDCG are quantified by global and local efficiency (GE and LE) [12, 13]. High global efficiency of one node shows that the node is connected to many nodes of the graph. Local efficiency of one node is high when the neighbors of this node are highly connected. GE and LE are calculated for all the nodes of positive and negative  $t$ -value graphs. The  $k$ -means method has been utilized to cluster the nodes (EEG electrodes) of the SDCG based on five features including GE, LE of positive and negative  $t$ -value graphs and power  $t$ -values. We can calculate the power of each electrode in IED and Non-IED time intervals in addition to correlations between the electrodes. Power  $t$ -values are results of MHT between the powers of IED and Non-IED time intervals in the related frequency band. The cluster related to the sources is labeled due to the physiological information about the patient.

### 3 Results and discussion

The proposed method has been applied on the real EEG data of epileptic patients. Please refer to [11] for the protocol of the data. The SDCG of a right frontal epilepsy has been shown in Fig. 2. Parts (a) and (b) show the positive and negative  $t$ -value SDCG respectively. Each connection in the positive (negative)  $t$ -value graph indicates the increase of wavelet correlations during IED (Non-IED) time intervals. The thickness of the connections is proportional to the absolute of  $t$ -values. The source cluster (obtained by  $k$ -means) has been shown in bold which demonstrates mostly the right and frontal electrodes. The source cluster is labeled due to the physiological information of the patient.

The electrodes near the source receive IED signals (volume conduction effect related to IED sources), hence the source electrodes (electrodes close to

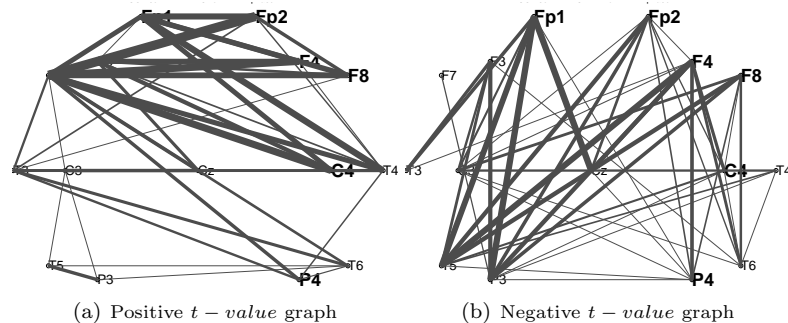


Fig. 2: Sparse differential connectivity graph (SDCG) for right frontal epileptic patient. (a) Positive  $t$ -value graph, (b) negative  $t$ -value graph. Connections of positive (negative)  $t$ -value graph shows that the wavelet correlations of IED (Non-IED) time intervals are significantly higher than Non-IED (IED) time intervals. The thickness of the connections are proportional to the absolute of  $t$ -values. The source cluster has been shown in bold.

the source) have high LE in positive  $t$ -value graph. Moreover, the GE of the source electrodes is high in negative  $t$ -value graph, since the correlation between electrodes far from the source and source electrodes decreases during IED time interval. Therefore, GE, LE of positive and negative  $t$ -value graphs and power  $t$ -values (Section 2) were selected to cluster the electrodes. The noise, artifact, background activity and their volume conduction effect were removed since SDCG indicates the connections whose wavelet correlations changing during IED and Non-IED time intervals. But the volume conduction of the IED sources exists which promotes clustering the source electrodes as described above. The validity of the results has been proven in a simulated data [14] in which the electrodes close to the true source were detected. This result in real data is in accordance with the expert neurologist witness.

Previous EEG connectivity studies suggested connectivity analysis on EEG activities (results of applying linear inverse problem). However any inverse problem method is based on some assumptions about the sources. The validity of the sources are dependent on these assumptions and the problem of volume conduction exists. To avoid these problems we applied connectivity analysis on the scalp EEG directly. However our aim is to study the brain functionality during epileptic and non-epileptic states of the brain to determine the related electrodes to the epileptiform sources from non-invasive EEG. This information is valuable for the intracranial electrode insertion. For precise seizure focus localization, we will apply the connectivity analysis on the intracranial EEG.

## 4 Conclusion

The proposed connectivity graph indicates the significant distinguished connections between two different brain states. By integrating complicated temporal information of EEG signal of the epileptic patient into a sparse differential connectivity graph and clustering the extracted features from the graph, we could determine the closer electrodes to the epileptiform sources.

## References

- [1] Y. A. L. Pijnenburg, R. L. M. Strijers, Y. v. Made, W. M. van der Flier, P. Scheltens, and C. J. Stam. Investigation of Resting-state EEG Functional Connectivity in Frontotemporal Lobar Degeneration. *Clinical Neurophysiology*, 119:1732–1738, August 2008.
- [2] S. Achard, R. Salvador, B. Whitcher, J. Suckling, and E. Bullmore. A Resilient, Low-Frequency, Small-World Human Brain Functional Network with Highly Connected Association Cortical Hubs. *The Journal of Neuroscience*, 26:63–72, 2006.
- [3] Gorsev Yener Bahar Guntekin, Ertugrul Saatci. Decrease of Evoked Delta, Theta and Alpha Coherences in Alzheimer Patients During a Visual Oddball Paradigm. *Brain Research*, In Press.
- [4] L. Astolfi, F. Cincotti, D. Mattia, F. De Vico Fallani, A. Tocci, A. Colosimo, S. Salinari, M. G. Marciani, W. Hesse, H. Witte, M. Ursino, M. Zavaglia, , and F. Babiloni. Tracking the Time-Varying Cortical Connectivity Patterns by Adaptive Multivariate Estimators. *IEEE Trans Biomed Eng.*, 55:902–13, 2008.
- [5] L. Astolfi, F. De Vico Fallani, F. Cincotti, D. Mattia, M. G. Marciani, S. Bufalari, S. Salinari, A. Colosimo, L. Ding, J. C. Edgar, W. Heller, G. A. Miller, B. He, and F. Babiloni. Imaging Functional Brain Connectivity Patterns From High-Resolution EEG and fMRI Via Graph Theory. *Psychophysiology*, 44:880–893, 2007.
- [6] D. Mantini, S. Cugini, G. L. Romani, and C. Del Gratta. Fusion of EEG and fMRI for the Investigation of Functional Connectivity During a Visual Oddball Task. *NFSI-ICFBI07*, pages 373–376, Oct. 2007.
- [7] D.B. Percival and A.T. Walden. Wavelet Methods for Time Series Analysis. *Cambridge, UK: Cambridge UP*, 2000.
- [8] L. Hudgings, C. Friehe, and M. E. Mayer. Wavelet Transforms and Atmospheric Turbulence. *Physics Review Letters*, 71:3279–3282, 1993.
- [9] A. Serroukh and A. T. Walden. Wavelet Scale Analysis of Bivariate Time Series I: Motivation and Estimation. 2000.
- [10] B. Whitcher, P. Guttorp, and D. Percival. Wavelet Analysis of Covariance with Application to Atmospheric Time Series. *Journal of Geophysical Research - Atmospheres*, 105:14941–14962, 2000.
- [11] L. Amini, R. Sameni, C. Jutten, G. A. Hossein-Zadeh, and H. Soltanian-Zadeh. MR Artifact Reduction in the Simultaneous Acquisition of EEG and fMRI of Epileptic Patients. In *Proc. of EUSIPCO08, Lausanne, Switzerland*, 2008.
- [12] D. J. Watts and S. H. Strogatz. Collective Dynamics of Small-world Networks. *Nature*, 393:440–442, 1998.
- [13] V. Latora and M. Marchiori. Economic Small-World Behavior in Weighted Networks. *Eur. Phys. J.*, 32:249–263, 2003.
- [14] D. Cosandier-Rim  l  , I. Merlet, J. M. Badier, P. Chauvel, and F. Wendling. The Neuronal Sources of EEG: Modeling of Simultaneous Scalp and Intracerebral Recordings in Epilepsy. *NeuroImage*, 42:135–146, 2008.